$Y$ = measurement matrix
$Z$ = matrix defined by Equation (23)
$z(j)$ = the $j$th column of $Z$

**Greek Symbols**

$\alpha$ = index characterizing the initial state
$\gamma(j)$ = the $j$th row of $T^{-1}$
$\epsilon$ = measurement error vector
$\lambda_j$ = the $j$th eigenvalue of $A$
$\mu_j(\lambda)$ = the $j$th eigenvalue of $Q(\lambda)$
$\mu(\lambda)$ = the smallest eigenvalue of $Q(\lambda)$, or as defined by Equation (25)
$\nu(\lambda)$ = the smallest eigenvalue of $W(\lambda)$
$\sigma$ = the error standard deviation
$\tau_1, \tau_2, \tau_3$ = time constants
$\tau_d$ = time delay

**Special Symbols**

$\wedge$ = indicates estimates
$o$ = indicates initial conditions
$T$ = as superscript indicates matrix transpose

**LITERATURE CITED**


Gavalas, G. R., and J. H. Seinfeld, "Estimation of the Volume of Reservoirs of Arbitrary Shape and Permeability Distribution," *J. Soc. Petr. Engrs*, submitted for publication.

Grabbe, E. M., S. Ramo, and D. E. Woodridge (eds.) *Handbook of Automation, and Control*, Vol. 3, pp. 9.05-9.08, Wiley, N. Y. (1961).

Nieman, R. E., D. G. Fisher, and D. E. Seborg, "A Review of Process Identification and Parameter Estimation Techniques," *Int. J. Control*, 13, 209 (1971).

Noble, B., *Applied Linear Algebra*, pp. 328-332, Prentice Hall, Englewood Cliffs, N. J. (1969).

Wei, J., and C. D. Prater, "The Structure and Analysis of Complex Reaction Systems," *Adv. Catalysis*, 13, 203 (1962).



*Manuscript received July 6, 1972; revision received August 30, 1972; paper accepted September 5, 1972.*


# Flow Rate-Pressure Gradient Measurements in Periodically Nonuniform Capillary Tubes


Flow rate-pressure gradient measurements have been performed on 15 different test capillary tubes, each of which consisted of short, alternating segments of two different diameters. The Reynolds number range covered extended from 2 to 700, based on the conditions in the narrower capillary segment. Darcy's law was found valid up to about $Re$ = 30-50, whereas the Forchheimer equation described the data over the entire range of $Re$ covered. The Forchheimer equation has been obtained from a nondimensional form of the volume averaged momentum equation by using the averaging theorem due to Slattery and to Whitaker. The parameters $\alpha$ and $\beta$ have obtained precise hydrodynamic definitions. The experimental data have been treated in terms of the Forchheimer equation: the parameters $\alpha$ and $\beta$ have been calculated using various definitions for the area of flow. Dimensionless permeability, equal to the ratio of measured-to-Poiseuille permeability has been found to be a minimum-type function of small-to-large capillary diameter ratio. Dimensionless inertial parameter $\beta^*$ has been found to be a maximum-type function of the capillary diameter ratio, if the calculation was based on the area of flow equal to the cross sectional area of the narrower capillary segment, in every case. The maximum occurred at the same value of the capillary diameter ratio as the minimum for the dimensionless permeability.



**FRANCIS A. L. DULLIEN**
**and**
**MOHAMED I. S. AZZAM**

**Department of Chemical Engineering**
**University of Waterloo**
**Waterloo, Ontario, Canada**


## SCOPE

It has been recognized for a long time that the flow channels (pores) in porous media contain constrictions and expansions, resulting in conical flow (for example, Scheidegger, 1957; Dullien and Batra, 1970) in the channels. The various expressions used to calculate permeabilities, however, usually neglect any effect conical flow may have on the permeability. Therefore, it seemed interesting to determine the magnitude of this effect experimentally. A highly simplified model of the flow channels in porous media has been chosen for this purpose, the permeability of which, excluding the effects of conical flow, could be calculated easily by the Hagen-Poiseuille equation. The measured permeability could then be compared with the predicted value, resulting in an estimate of the magnitude of excess viscous dissipation due to the existence of convergent-divergent flow in the capillaries. The model used

in this work has been a single capillary tube consisting of alternating short pieces of individual capillaries of three different diameters. Fifteen combinations of capillary diameters and lengths have been used. The axial cross section of the test capillary tubes had the shape of a square wave. It is realized that flow channels in actual porous media have far more irregular shapes, so that the findings of this work may have only qualitative or, at best, semiquantitative implications for the interpretation of flow phenomena in porous media. It is not presumed in the least that a capillary tube may be endowed with the many various properties of a porous medium. At most, the test capillary used in this work may be regarded as a rather special model of an individual flow channel or pore such as there are in porous media. On the other hand, it is conceivable to imagine various models of a porous medium containing capillaries similar to those used in the present work. The simplest of these models would contain identical, parallel capillary tubes imbedded in some impervious solid. This would amount to a special case of the well-known, serial type capillaric model, (for example, Scheidegger, 1957). Hence, the test capillaries used in this study may form building blocks of models of porous media. Since it is convenient to discuss the results of this work in terms of concepts borrowed from the field of flow through porous media, for example, permeability, it might be helpful to visualize the test capillary imbedded in an impervious solid with a total cross-sectional area $A$. It might even be better to visualize the above serial type capillaric model, containing many parallel test capillaries imbedded in the solid, with an average cross-sectional area $A$ per capillary tube. These models might make the transition easier from a single test capillary to the concept of a porous medium, however special that may be.

## CONCLUSIONS AND SIGNIFICANCE

1. The Forchheimer equation has been obtained by applying the averaging theorem due to Slattery and to Whitaker to the volume averaged nondimensional momentum equation. As a result, precise hydrodynamic definitions have been obtained for the reciprocal permeability $\alpha$, and the inertial parameter $\beta$.

2. Flow rate-pressure drop measurements have been performed on a set of 15 straight test capillaries, one at a time, each of which consisted of alternating short pieces of individual segments of two different inside diameters. The measurements extended over a range of Reynolds numbers from 2 to 700, based on the diameter of, and the velocity in, the smaller hole in every case.

3. The data were treated in terms of the Forchheimer relation. Up to about 30-50 $Re$ Darcy's law held, and the quadratic term could be neglected. The permeabilities have been obtained both from the low Reynolds number region and also from the higher Reynolds number region with satisfactory agreement between the results. The Forchheimer relation accurately represented all the data. $\beta$ was also determined for each test capillary tube.

4. Dimensionless permeabilities and dimensionless inertial parameters of the test capillaries are functions only of the small-to-large capillary diameter ratio and the capillary diameter-to-wave-length ratio.

5. Dimensionless permeabilities, equal to the ratio: measured permeability-to-Poiseuille permeability were calculated and plotted versus small-to-large capillary diameter ratio, with the capillary diameter-to-wave-length ratio as parameter. The dimensionless permeabilities varied from unity, corresponding to a uniform capillary, through values as low as about 0.4, back to unity again when the capillary diameter ratio became very small.

6. The inertial parameter, both in the dimensional and the nondimensional form, has been found to be a very different function of the capillary diameter ratio, depending on the choice of the area of flow on which the value of $v$ has been based. When basing $v$ on the area of flow in the smaller capillary in every case, the plot of $\beta$ versus capillary diameter ratio had a pronounced maximum at the same value of the diameter ratio for which the dimensionless permeability had a minimum.

7. The value of $\beta$, based on the area of flow corresponding to the constrictions of the flow channels or pores in porous media may be expected to represent the relative magnitudes of the inertial effects more accurately than the value based on the filter velocity $q$. The average value of the throat-to-void diameter ratio in the medium may be determined by a comparison of mercury porosimetry and photomicrographic pore size distribution curves, and the throat velocity may be estimated from $q$, using this ratio and the porosity.

### EXPERIMENT

The individual test capillaries consisted of assemblages of $3.175 \times 10^{-3}$ m thick acrylic discs, each disc having a hole drilled in the center with a minimum tolerance of about $1 \times 10^{-5}$ m. In every test, capillary discs with two different hole diameters were used, and the different discs were arranged periodically as ABABAB..., or AABBAABB..., or AAAABBBBAAAABBBB.... 28 discs of each kind were normally used, resulting in a test capillary $17.8 \times 10^{-2}$ m long. Four different hole diameters, $4.3 \times 10^{-4}$ m, $8.3 \times 10^{-4}$ m, $34.3 \times 10^{-4}$ m, and $46 \times 10^{-4}$ m were used. Five different combinations of diameters have been used. Thus, the total number of different test capillaries was fifteen.

The construction of a typical disc is shown in Figure 1. In one face of each disc a concentric slot was machined which served as a seat for an O-ring. The discs were stacked inside a Plexiglas tube, which was equipped with the necessary means to achieve satisfactory alignment and tightening of the discs (Azzam, 1971). Suitable end pieces provided connections to the manometer. Two U-tube manometers were used, one at a time, depending on the conditions of the experiment. One was 1.20 m, with mercury as the manometer liquid, the other was 0.65 m, and the manometer liquid was Merium Oil of specific gravity equal to 2.95. A Mariotte's bottle type constant head tank was used. Flow rates were obtained by collecting samples over a certain convenient period of time (usually 10 min. or longer), and weighed.

Accurate dimensions of the holes in the discs, and perfect alignment of the holes were of vital importance for obtaining meaningful data. Therefore all measurements of the discs were checked under a light projector, after machining and the tolerances were found to be better than $\pm 1 \times 10^{-5}$ m. The effect of alignment was checked by restacking the discs. Good repro-

ducibility was always obtained. Air bubbles were removed by a water aspirator before starting a run. End effects were checked out by running tests also with shorter stacks of discs in every case. Within experimental error, the same pressure gradient always resulted in the same flow rate in identical tubes of different lengths.

A typical set of raw data is shown in Figure 2. It can be seen that at sufficiently low pressure gradients the flow rate is a *linear function of* pressure gradient, but at higher values the slope of the line starts to decrease gradually. The Reynolds number range covered in the case of each tube was about 2-700, based on the diameter of, and the velocity in, the smaller hole in every case. Darcy's law started to break down in the range of Reynolds number 30-50, in all the tubes tested. Literature data (for example, Katz, 1959) on unconsolidated sands indicated that deviations from Darcy's law begin to show up in the range of *Re* 7-10, where the Reynolds number was based on the average grain diameter and the apparent velocity = volumetric flow rate/cross-sectional area. Evidently a Reynolds number calculated in this fashion is smaller than the one based on the diameter of and flow velocity in the constrictions of the flow channels. Had the Reynolds numbers in Katz (1959) been calculated in this fashion, it is likely that deviations from Darcy's law in unconsolidated sands would have started to show up at Reynolds numbers closer to the values found in the present study.

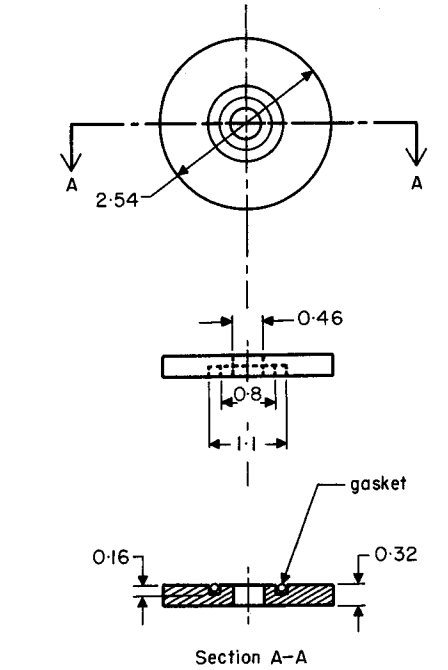


**Fig. 1. Constructional details of a disc.**

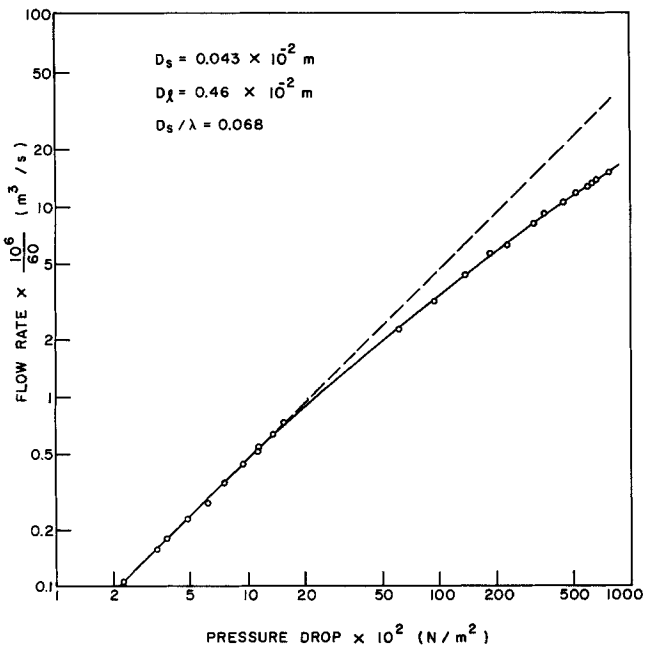


**Fig. 2. Sample plot showing complete range of raw data for one of the tubes.**

## THEORY

The familiar Forchheimer equation has been used to fit the flow rate-pressure gradient data lying outside the range of validity of Darcy's law (Scheidegger, 1957; Katz, 1959). The Forchheimer equation is basically an empirical curve fit (Scheidegger, 1957) which has been used mostly with a second-order term in the velocity, but sometimes a third-order term has also been added. Therefore, it has been of some interest to examine what the correct form of a general relation between the pressure gradient and velocity in porous media can be expected to be from basic principles. As a result of the development given in detail below, the parameters of the Forchheimer equation obtained precise hydrodynamic definitions.

Although in the present study the Forchheimer equation has been used to fit the pressure gradient-velocity data obtained in single test capillary tubes, it would have been an unnecessary limitation to restrict the scope of the analysis to this special type of system. Hence, the development is presented for the general case of any rigid porous medium. The results also apply to the data obtained in the present study. In order to see this one might want either to imagine an artificial porous medium consisting of many identical, parallel test capillary tubes imbedded in an impervious solid or to go over the development of the Forchheimer equation given below and become convinced that the result of the analysis is equally valid for a single test capillary tube.

### Development of the Forchheimer Equation

The microscopic equation of conservation of momentum for an isothermal system is

$$\frac{\partial}{\partial t}\rho \mathbf{u} = -\underline{\nabla}\cdot\rho\,\mathbf{u}\,\mathbf{u} - \underline{\nabla}p - \underline{\nabla}\cdot\underline{\tau} + \rho\,\mathbf{g} \qquad (1)$$

Assuming that the flow is steady, turbulence effects are negligible, and the fluid is Newtonian with constant physical properties, Equation (1) reduces to

$$0 = -\rho\,\mathbf{u}\cdot\underline{\nabla}\mathbf{u} - \underline{\nabla}P + \mu\,\nabla^2\mathbf{u} \qquad (2)$$

where

$$P = p - p_0 + \rho\,\phi \qquad (3)$$

with $p_0$ being some reference pressure and $\phi$ the gravitational potential function which satisfies the equation

$$\mathbf{g} = -\underline{\nabla}\,\phi \qquad (4)$$

Let us choose some reference magnitudes of length ($D$) and speed ($v$) which are characteristic of the system. Clearly the choice of these magnitudes is arbitrary. It is useful, however, to select for $D$ some characteristic diameter of the flow channels, and use the magnitude of some average flow velocity in the flow channels for $v$. Then Equation (2) can be rewritten

$$0 = -\frac{\rho v^2}{D}\mathbf{u}^* \cdot \underline{\nabla}^* \mathbf{u}^* - \frac{\rho v^2}{D}\underline{\nabla}^* P^* + \frac{\mu v}{D^2}\nabla^{*2}\mathbf{u}^* \tag{5}$$

where

$\mathbf{u}^* = \mathbf{u}/v$; $P^* = P/\rho v^2$; $\underline{\nabla}^* = D\,\underline{\nabla}$; and $\nabla^{*2} = D^2\nabla^2$.

Next, Equation (5) is averaged over a volume $V$ that is constant, and its orientation relative to some inertial frame remains unchanged. Other restrictions are that $D << l << L$, where $l$ is a characteristic length for $V$, and $L$ some macroscopic dimension representative of the process under consideration. The physical meaning of forming volume averages in a porous medium has been discussed in detail by Whitaker (1969).

$$\frac{\rho v^2}{D}\frac{1}{V}\int_{V_f}\underline{\nabla}^* P^*\,dV = \frac{\mu v}{D^2}\frac{1}{V}\int_{V_f}\nabla^{*2}\mathbf{u}^*\,dV - \frac{\rho v^2}{D}\frac{1}{V}\int_{V_f}\mathbf{u}^*\cdot\underline{\nabla}^*\mathbf{u}^*\,dV \tag{6}$$

where $V_f$ is the portion of $V$ occupied by fluid. Applying the divergence theorem to the volume average pressure gradient on the left-hand side of the last equation

$$\frac{1}{V}\int_{V_f}\underline{\nabla}^* P^*\,dV = \frac{1}{V}\int_{A_w} P^*\,\mathbf{n}\,dA + \frac{1}{V}\int_{A_e} P^*\,\mathbf{n}\,dA \tag{7}$$

where $A_e$ represents the area of the entrances and exits on the surface $A$, and $A_w$ represents the area of the solid-fluid interface contained within $V$. Naturally

$$A_w + A_e = A_f \tag{8}$$

where $A_f$ is the area of the boundary surface of $V_f$.

Applying to $P^*$ Slattery's averaging theorem (5) as presented by Whitaker (1969)

$$\underline{\nabla}^*\langle P^*\rangle = \frac{1}{V}\underline{\nabla}^*\int_{V_f} P^*\,dV = \frac{1}{V}\int_{A_e} P^*\,\mathbf{n}\,dA \tag{9}$$

where $\langle\ \rangle$ denote volume averages. Combining Equations (9) and (7) and introducing the result into Equation (6) yields

$$\frac{\rho v^2}{D}\left(\underline{\nabla}^*\langle P^*\rangle + \frac{1}{V}\int_{A_w} P^*\,\mathbf{n}\,dA\right) = \frac{\mu v}{D^2}\frac{1}{V}\int_{V_f}\nabla^{*2}\mathbf{u}^*\,dV - \frac{\rho v^2}{D}\frac{1}{V}\int_{V_f}\mathbf{u}^*\cdot\underline{\nabla}^*\mathbf{u}^*\,dV \tag{10}$$

Using the definition of $P^*$ and $\nabla^*$, one has

$$\underline{\nabla}^*\langle P^*\rangle = \frac{D}{\rho v^2}\underline{\nabla}\langle P\rangle \tag{11}$$

Inserting this expression into Equation (10) gives, after solving for $\underline{\nabla}\langle P\rangle$,

$$\underline{\nabla}\langle P\rangle = \mu v\left[\frac{1}{D^2}\frac{1}{V}\int_{V_f}\nabla^{*2}\mathbf{u}^*\,dV\right] + \rho v^2\left[-\frac{1}{D}\frac{1}{V}\int_{V_f}\mathbf{u}^*\cdot\underline{\nabla}^*\mathbf{u}^*\,dV - \frac{1}{D}\frac{1}{V}\int_{A_w} P^*\,\mathbf{n}\,dA\right] \tag{12}$$

Equation (12) has the same form as the Forchheimer equation with the bracketed term, coefficient of $v$, being the reciprocal permeability $\alpha$ and the other bracketed expression, coefficient of $v^2$, being the inertial parameter $\beta$:

$$\underline{\nabla}\langle P\rangle = \alpha\,\mu v + \beta\,\rho v^2 \tag{13}$$

In the range of validity of the Forchheimer equation, $\alpha$ and $\beta$ are constants by definition. At low velocities such that $v^2 << v$, Equation (12) reduces to Darcy's law. A sufficient condition for the constancy of $\alpha$ is that the velocity $\mathbf{u}$ at a fixed point be proportional to $v$. This condition, however, is not sufficient for the constancy of $\beta$, unless the second term in the bracketed expression defining $\beta$ is negligible compared with the first term. If it is permissible to generalize the known relations existing in some simple problems of fluid flow, the proportionality between $\mathbf{u}$ and $v$ may be expected to hold in low Reynolds number flow. The physical interpretation given to $\alpha$ and $\beta$ in the above treatment [Equation (12)] is worth noting. It is evident that $\alpha$ is proportional to the volume averaged dimensionless Laplacian of the dimensionless velocity $\mathbf{u}^*$, whereas $-\beta$ is proportional to the algebraic sum of the volume averaged convective acceleration, and the dimensionless pressure force, per unit volume, acting on the solid-fluid interface. For laminar flow in a straight cylindrical capillary the definition of $\beta$ contained in Equation (12) gives immediately $\beta = 0$. An easy calculation yields for $\alpha$ the well-known result $\alpha = 32/D^2$.

## TREATMENT AND DISCUSSION OF RESULTS

The empirical relationships used in problems of flow through porous media, such as Darcy's law and the Forchheimer equation, are usually based on the total cross-sectional area of the porous medium, which includes the cross section of a varying proportion of impervious solid associated with the pores. While it has been generally realized that the filter velocity $q$ defined by this cross-sectional area tends to be smaller than any kind of average velocity in the flow channels, so-called "pore velocity" $v$ (Scheidegger, 1957; Guin et al., 1971), the use of $q$ has great practical advantages, one of them being the fact that the total cross-sectional area usually is well-defined and readily measurable. It is easy to allow for the presence of solids by dividing $q$ with the porosity $\phi$ to obtain $v$ (Dupuis-Forchheimer assumption), but the resulting pore velocity is unequivocally correct only for the case of uniform pores (Guin et al., 1971).

In the case of the test capillaries used in this study there was no obvious, natural cross-sectional area on which to base the calculation of the flow velocity. For a direct comparison of the permeabilities of the 15 different test capillaries, the flow cross section $A = 10^{-4}$ m$^2$ seemed most convenient. The permeabilities calculated in this manner are shown in column 5 of Table 1. Supposing that in the case of every different test capillary tube, an artificial porous medium, containing parallel capillary tubes imbedded in an impervious solid is visualized, the choice $A = 10^{-4}$ m$^2$ would mean that the total cross-sectional area of the medium divided by the number of parallel tubes is equal to $10^{-4}$ m$^2$, in each case. There would follow from this that each of these artificial porous media would have a different porosity.

Depending on one's point of view, it may appear artificial to some to assign a certain amount of impervious solid to every test capillary tube. It might seem preferable to base the average flow velocity on some intrinsic cross section of the test capillary. Several of such choices are possible, including the volume average cross-sectional area, $(A_s + A_l)/2$, and the cross section $A_s$ of the narrower of the two capillary segments, in every case. The former choice of cross section corresponds to the Dupuis-Forch-

Table 1. Dimensions and Permeabilities of Test Capillary Tubes

| $D_s \times 10^{-2}$ (m) | $D_l \times 10^{-2}$ (m) | $D_s/D_l$ | $D_s/\lambda$ | Permeability $\times 10^4$ ($m^2$) Based on $A = 10^{-4}$ $m^2$ Darcy's law region $\times 10^{-7}$ | Based on the cross section $A_s$ of the narrower capillary Darcy's law region $\times 10^{-5}$ | Inertial region $\times 10^{-5}$ |
|---|---|---|---|---|---|---|
| 0.043 | 0.46 | 0.094 | 0.068 | 1.4 | 9.6 | 9.1 |
| 0.043 | 0.46 | 0.094 | 0.034 | 1.6 | 11.0 | 11.0 |
| 0.043 | 0.46 | 0.094 | 0.017 | 1.65 | 11.5 | 12.0 |
| 0.043 | 0.343 | 0.126 | 0.068 | 1.2 | 8.0 | 8.3 |
| 0.043 | 0.343 | 0.126 | 0.034 | 1.3 | 8.6 | 9.0 |
| 0.043 | 0.343 | 0.126 | 0.017 | 1.4 | 9.6 | 9.7 |
| 0.083 | 0.46 | 0.18 | 0.132 | 4.7 | 8.7 | 9.1 |
| 0.083 | 0.46 | 0.18 | 0.066 | 5.7 | 10.5 | 9.1 |
| 0.083 | 0.46 | 0.18 | 0.033 | 7.5 | 14.0 | 13.0 |
| 0.083 | 0.343 | 0.24 | 0.132 | 7.6 | 14.1 | 16.2 |
| 0.083 | 0.343 | 0.24 | 0.066 | 9.2 | 17.1 | 19.8 |
| 0.083 | 0.343 | 0.24 | 0.33 | 11.3 | 21 | 24.3 |
| 0.043 | 0.083 | 0.52 | 0.068 | 0.95 | 6.6 | 6.7 |
| 0.043 | 0.083 | 0.52 | 0.034 | 1.1 | 7.6 | 7.3 |
| 0.043 | 0.083 | 0.52 | 0.017 | 1.25 | 8.6 | 9.6 |

heimer definition of pore velocity, whereas the latter will evidently yield the highest value of the area-average flow velocity in the capillary tubes.

### Treatment of Experimental Data in Terms of the Forchheimer Relation

As it is apparent from Figure 2, showing a typical set of raw data, the flow measurements have been taken over a wide range of Reynolds numbers. Plotting the data according to Equation (13) in the form

$$\frac{\Delta p}{l}\frac{1}{\mu v} = \alpha + \beta\frac{\rho}{\mu}v \qquad (14)$$

straight lines were obtained. $\alpha$ was obtained from the $v = 0$ intercept and $\beta$ from the slope of the line. The calculations have been performed for two different choices of area of flow: (1) The cross sectional area $A_s$ of the smaller hole, and (2) the volumetric mean cross sectional area $(A_s + A_l)/2$. For the first choice of area of flow, the permeabilities have been calculated also from the data taken at very low flow rates, when Equation (13) reduces to Darcy's law, and we have

$$\frac{\Delta p}{l} = \alpha\mu v \qquad (15)$$

The two sets of permeabilities, calculated from Equations (14) and (15), respectively agreed within experimental errors, and they are shown in columns 6 and 7 of Table 1. Typical examples of the plots based on Equations (15) and (14) are shown in Figures 3 and 4, respectively.

### Correlation of Measured Permeabilities and Inertial Parameters in Terms of Geometry of Test Capillaries

Considering the definitions of $\alpha$ and $\beta$ [Equation (12),] Equation (14) can be written as follows:

$$1 = \left(\frac{\mu v}{D^2}\frac{l}{\Delta p}\right)\alpha^* + \left(\frac{\rho v^2}{D}\frac{l}{\Delta p}\right)\beta^* \qquad (16)$$

Equation (16) gives a relationship between the four dimensionless groups $\frac{\mu v}{D^2}\frac{l}{\Delta p}$, $\alpha^*$, $\frac{\rho v^2}{D}\frac{l}{\Delta p}$, and $\beta^*$. In the range of validity of the Forchheimer relation where $\alpha$ and $\beta$ are independent of $v$, it follows from Equation (12) that the groups $\alpha^* = \alpha D^2$ and $\beta^* = \beta D$ are functions only of the proportions of the flow channels. In the case of the test capillaries used in the present work the proportions of the flow channels may be characterized by the two independent dimensionless ratios, the ratio of the small hole diameter to the large hole diameter $D_s/D_l$ and the ratio of the small hole diameter to the wave length (the length of a period in the test capillary, consisting of two discs, one with a small hole and the other with a large one) $D_s/\lambda$. Hence, one can write

$$\alpha^* = \alpha^*\left(\frac{D_s}{D_l}, \frac{D_s}{\lambda}\right), \text{ and } \beta^* = \beta^*\left(\frac{D_s}{D_l}, \frac{D_s}{\lambda}\right) \qquad (17a, b)$$

There follows then that in the case of the present test capillaries Equation (16) is in fact, a relation between

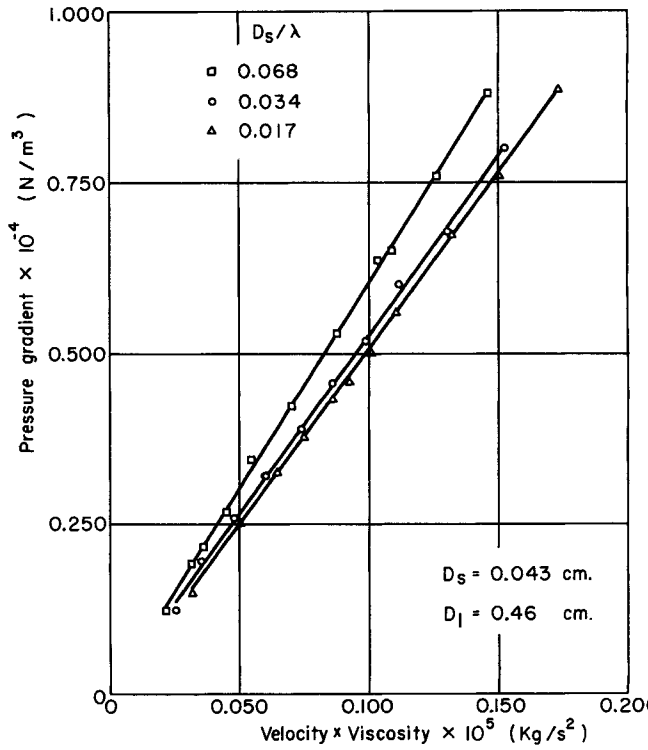


Fig. 3. Sample plot at low velocities (Darcy's law region). Velocity is based on volume average area of flow.

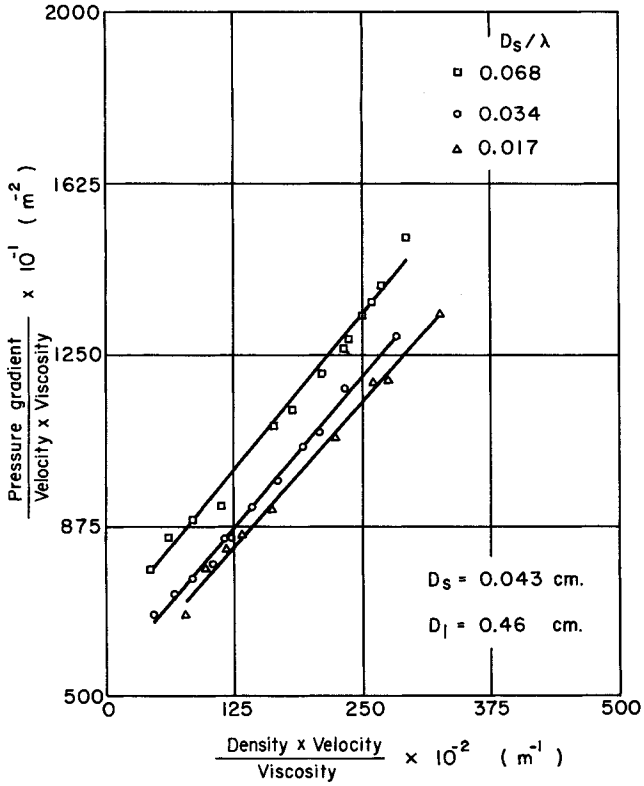


**Fig. 4. Sample plot of Forchheimer equation at higher velocities. Velocity is based on volume average area of flow.**

the dimensionless groups $\frac{\mu v}{D^2}\frac{l}{\Delta p}$, $\frac{\rho v^2}{D}\frac{l}{\Delta p}$, $\frac{D_s}{D_l}$, and $\frac{D_s}{\lambda}$. This is consistent with the results of a dimensional analysis performed on the test capillary.

1. Correlation of $1/\alpha^*$ with $D_s/D_l$ and $D_s/\lambda$

In calculating $\alpha^*$ from $\alpha$, the choice of the characteristic diameter $D$ is arbitrary. It is useful, however, in this case to select $D$ such that it will give for $1/\alpha^*$ the ratio of measured-to-Poiseuille permeability. By the latter is meant the permeability of the test capillary one would calculate by assuming the validity of the Hagen-Poiseuille equation inside each capillary segment, and neglect all other dissipation effects.

It is perhaps best to return at this point to the measured flow rate $Q$, which is devoid of any arbitrarily assigned flow cross section, or diameter. The measured permeability $k_m$ is, of course, defined by Darcy's law

$$\frac{1}{\alpha} = k_m = \frac{Q\mu}{A(\Delta p/l)} \tag{18}$$

where $Q$, $\mu$, and $\Delta p/l$ are experimental quantities and $A$ is an arbitrary flow cross section. The calculated permeability, obtained by using the Hagen-Poiseuille equation, is

$$k_c = \frac{Q_{\text{H.P.}}\,\mu}{A(\Delta p/l)} \tag{19}$$

where $Q_{\text{H.P.}}$ is the flow rate in the test capillary calculated by the Hagen-Poiseuille equation for the same values of $\mu$ and $(\Delta p/l)$ as in Equation (18). The flow cross section $A$ in Equation (19) is also the same value as in Equation (18).

For steady flow through the test capillary

$$Q_{\text{H.P.}} = \frac{\Pi D_s^4}{128\,\mu}\frac{\Delta p_s}{\lambda/2} = \frac{\Pi D_l^4}{128\,\mu}\frac{\Delta p_l}{\lambda/2} \tag{20}$$

The pressure drop $\Delta p$ over the total length $l = m\lambda$ of the tube is

$$\Delta p = m(\Delta p_s + \Delta p_l) = \frac{64\mu Ql}{\Pi}\left(\frac{1}{D_s^4} + \frac{1}{D_l^4}\right) \tag{21}$$

whence

$$Q_{\text{H.P.}} = \frac{\Pi}{64\,\mu\left(\frac{1}{D_s^4} + \frac{1}{D_l^4}\right)}\frac{\Delta p}{l} \tag{22}$$

Insertion of Equation (22) into Equation (19) gives

$$k_c = \frac{\Pi}{64\,A\left(\frac{1}{D_s^4} + \frac{1}{D_l^4}\right)} \equiv D^2 \tag{23}$$

Finally, by forming the ratio $k_m/k_c$, the following expression is obtained from Equations (18) and (23)

$$\frac{1}{\alpha^*} = \frac{k_m}{k_c} = \frac{64Q\mu}{\Pi(\Delta p/l)}\left(\frac{1}{D_s^4} + \frac{1}{D_l^4}\right) \tag{24}$$

Equation (24) is the desired expression for $1/\alpha^*$. It is noted that there is no arbitrary flow cross section in Equation (24). Hence, this is a true measure of the excess dissipation effects which took place in the test capillaries and which are not taken into account by the H.P. equation.

$k_m/k_c$ has been plotted versus $D_s/D_l$, with $D_s/\lambda$ as a parameter in Figure 5. As it can be seen from the data in Table 1, the permeabilities obtained from low Reynolds number measurements by Equation (15) agreed with the corresponding permeabilities obtained from measurements made at higher Reynolds numbers by Equation (14) within experimental errors. Nevertheless in Figure 5 the low Reynolds number measurements have been used because they were considered more reliable.

It is noted that for a tube of uniform diameter the measured permeability is equal to the calculated one; hence for $D_s/D_l = 1$ there follows $k_m/k_c = 1$. At the other extreme, when $D_s/D_l << 1$, one might argue intuitively that the entire pressure drop is expected to occur in the narrow capillary segments. Since this is also what the Hagen-Poiseuille equation predicts, one might expect that for

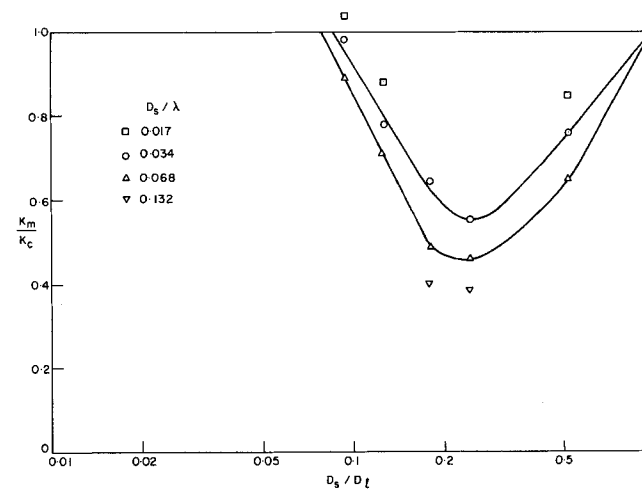


**Fig. 5. Effect of diameter ratio and wavelength on permeability.***

* Permeabilities were calculated from low Reynolds number measurements, using Darcy's law. Within experimental errors the same permeabilities were obtained from high Reynolds number measurements, using the Forchheimer equation.

very low values of $D_s/D_l$ the ratio $k_m/k_c$ is again equal to 1. It is apparent from the graph in Figure 5 that for the lowest value of $D_s/D_l$ covered in this study (0.1), $k_m/k_c$ is approaching unity. The fact that one of the points lies at about $k_m/k_c = 1.04$ can be accounted for by the stated tolerance of $D_s$, which is about $\pm 1 \times 10^{-5}$ m. Assuming that $D_s$ is not $4.3 \times 10^{-4}$ m but $4.4 \times 10^{-4}$ m, one obtains by Equation (24) 0.92 instead of 1.04, for $k_m/k_c$. Hence, this particular value of $k_m/k_c$ is equal to 1.0 within experimental error.

In between the two extremes where $k_m/k_c = 1$, the value of this ratio is less than one, and it appears to have a pronounced minimum at about $D_s/D_l = 0.25$. When trying to give at least a reasonable qualitative explanation for the observed behavior, it should be born in mind that in the present experiments the least value of the length-to-diameter ratio of the narrower capillary segments was 3.8, whereas for the larger capillary segments the same ratio was always much smaller, in many cases less than one. Therefore, it seems likely that end effects played a far smaller role in the narrower segments than in the larger ones. Assuming that most of the excess viscous dissipation took place in the larger capillary segments, the development of a minimum in the $k_m/k_c$ versus $D_s/D_l$ curves can be expected to be due to a variation with $D_s/D_l$ of the magnitude of the velocity gradients in the larger segments. When $D_s/D_l$ is close to one, the velocity changes between the two capillaries of different diameters are small, and the velocity gradients caused by the changing boundaries are small, too. With decreasing $D_s/D_l$ the bulk velocity changes increasingly between the two capillaries. It appears, however, that big velocity gradients are set up only as long as the walls of the larger capillary segment are not too far removed. It is the presence of these walls that makes the direction and magnitude of the point velocities change rather abruptly and causes excess viscous dissipation thereby. When the walls are far away, that is, $D_s/D_l << 1$, the magnitude of the velocity near the solid is practically zero everywhere, and the changes in the direction and magnitude of the point velocities may take place very gradually so that the amount of viscous dissipation caused by the changing boundaries becomes very small.

The dependence of $k_m/k_c$ on $D_s/\lambda$ is moderate and follows the expected pattern, that is, $k_m/k_c$ increases with decreasing $D_s/\lambda$.

2. Correlation of $\beta^*$ with $D_s/D_l$ and $D_s/\lambda$

In the case of the inertial parameter $\beta$, the diameter corresponding to the area of flow used in calculating $v$ was used also for $D$ in the relation $\beta^* = \beta D$.

As pointed out above, $\beta$ has been calculated for two different choices of area of flow: the volumetric mean area $(A_s + A_l)/2$ and the smaller area $A_s$. The plots of $\beta^*$ for these two choices of the area of flow are shown versus $D_s/D_l$, with $D_s/\lambda$ as parameter in Figures 6 and 7. As it is apparent from the graphs, not only is the absolute value of $\beta^*$ greatly dependent upon the choice of area of flow, but, more importantly, the dependence on $D_s/D_l$ is also very strongly affected by this choice. If the volume average area of flow is used, $\beta^*_{\text{vol.av.}}$ (and also $\beta_{\text{vol.av.}}$) drops monotonously and rapidly with increasing $D_s/D_l$, thereby creating an impression of decreasing magnitude of inertial effects. The volumetric mean area of flow differs from the cross-sectional area used to calculate filter velocities $q$ only by the porosity as a factor, that is, $v_{\text{vol.av.}} = q/\phi$, where $\phi$ is the porosity. Hence, the value of $\beta$ based on filter velocities can be expected to decrease with increasing $D_s/D_l$ for different porous media of approximately the same porosity. By contrast, when using $v$ based on the

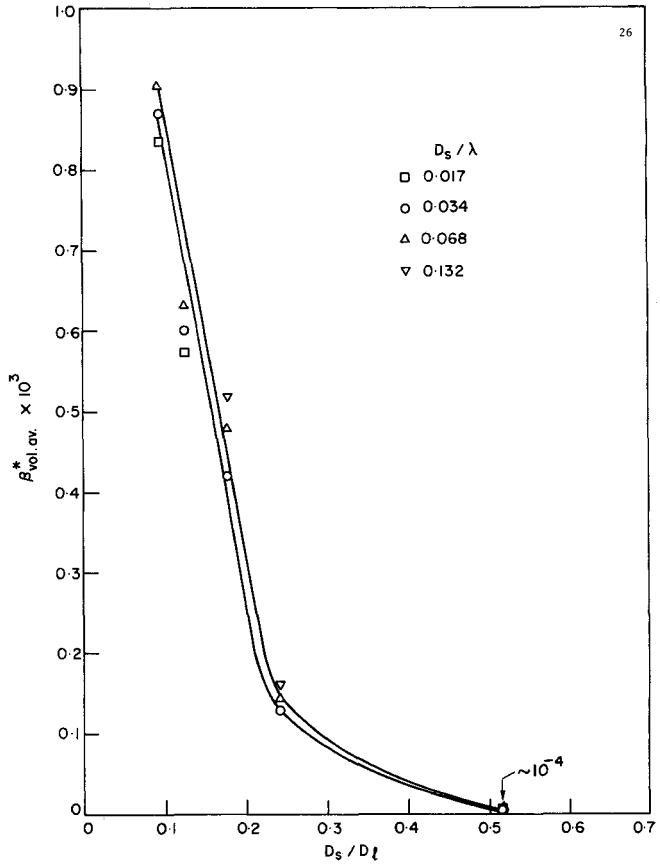


Fig. 6. Effect of diameter ratio and wave length on inertial parameter $\beta^*_{\text{vol.av.}}$

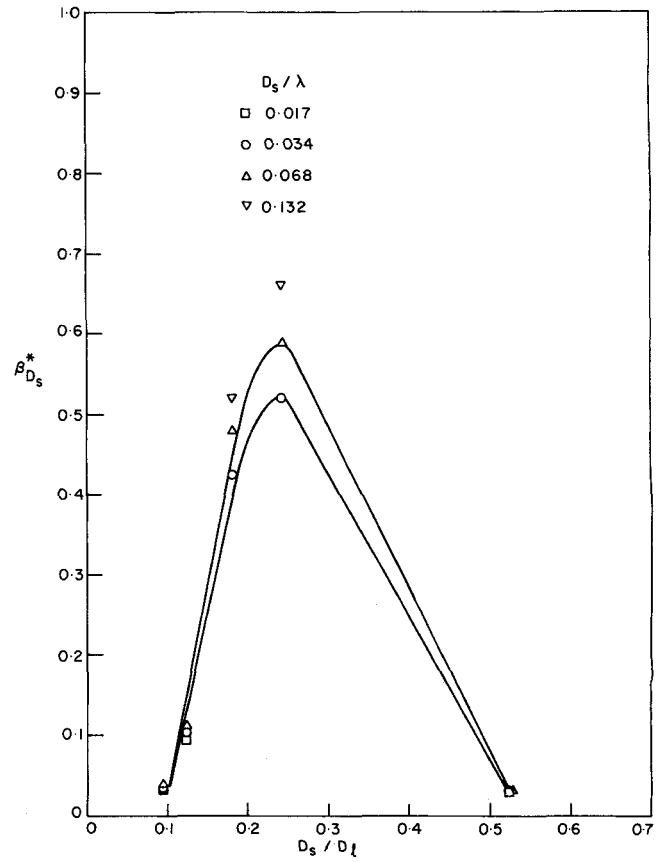


Fig. 7. Effect of diameter ratio and wavelength on inertial parameter $\beta^*_{D_s}$.

small area of flow $A_s$, the value of $\beta^*_{D_s}$ (and also $\beta_{D_s}$) varies with $D_s/D_l$ in an altogether different fashion: it has a pronounced maximum at $D_s/D_l \approx 0.25$, the same value where $k_m/k_c$ has a minimum. This kind of variation of $\beta^*_{D_s}$ with $D_s/D_l$ suggests that the magnitude of inertial effects is small not only when $D_s/D_l$ is approaching unity, but also when this ratio is very small. The fact of the matter is that inertial effects may indeed be expected to have a maximum at the same value of $D_s/D_l$ where $k_m/k_c$ has a minimum.

The results of this work may be applied to the interpretation of flow phenomena in actual porous media only with great caution. In the present study, only one of the characteristics of flow channels (pores) in porous media has been studied in isolation. Whereas this property, the variation in the cross section of flow channels, is probably an important one, there are quite a few more which also require detailed study, including the interconnectedness of the pores in actual porous media. Since the excess viscous dissipation has been found in this study to be a relatively weak function of the wave length, it seems not unreasonable to assume that the excess dissipation would be not greatly different if the narrow and the large capillaries had unequal lengths. In actual porous media the shapes of flow channels are generally irregular and not the square-wave type which were studied in this work. Therefore, the findings of this study may have only qualitative implications for porous media. It seems a reasonable supposition, however, that if $\beta$ were calculated using pore velocities based on the area of flow of the throats (or necks) of flow channels in porous media, it might be a more nearly accurate measure of the magnitude of inertial effects. This, of course, can be done only approximately, and only if there is some information available on the average value of $D_s/D_l$ in the sample. Estimates of average values of $D_s$ and $D_l$ may be obtained from mercury porosimetry and photomicrographic pore size distribution curves of the sample. The two techniques have been used jointly recently by Dullien et al. (1969/70, 1971, 72, 1972), who have also demonstrated the applicability of quantitative photomicrographic work to pore size distribution determinations. There seems to be some incentive to determine $\beta_{D_s}$ and $\beta^*_{D_s}$, as well as $k_m/k_c$, in various porous media in an attempt to improve our understanding of the relationship between flow phenomena and pore structure.


## ACKNOWLEDGMENTS

Grants-in-Aid by the National Research Council of Canada and by the University of Waterloo are greatly appreciated by the authors, who are also indebted to Dr. J. E. Lewis for his help in the experimental part of this work. F. A. L. Dullien wishes to acknowledge helpful discussions with Professor R. A. Greenkorn and T. G. Theofanous.


## NOTATION

$A$ = surface of the averaging volume; area of flow
$A_e$ = area of entrances and exits of $A_f$
$A_f$ = surface of the fluid volume contained within the averaging volume
$A_w$ = area of solid-fluid interface of $A_f$
$D$ = characteristic length for the structure of the porous medium; diameter of capillary
$g$ = gravitational acceleration
$k$ = permeability
$L$ = macroscopic dimension representative of the process under consideration
$l$ = length of test capillary tube; a characteristic length for the averaging volume
$m$ = number of periods in test capillary = number of small capillary segments = number of large capillary segments
$\mathbf{n}$ = outwardly directed unit vector normal to surface
$P$ = piezometric pressure, Equation (3)
$P^*$ = $P/\rho v^2$ = dimensionless piezometric pressure
$p$ = pressure
$p_0$ = reference pressure
$Q$ = volumetric flow rate
$Q_{H.P.}$ = volumetric flow rate calculated by the Hagen-Poiseuille equation
$q$ = $Q/A$ = filter velocity
$t$ = time
$\mathbf{u}$ = velocity vector
$\mathbf{u}^*$ = $\mathbf{u}/v$ = dimensionless velocity vector
$V$ = averaging volume
$V_f$ = fluid volume contained within the averaging volume
$v$ = characteristic average speed of the fluid in the porous medium

### Greek Letters

$\alpha$ = parameter in the Forchheimer equation [Equations (12) and (13)]; reciprocal of permeability
$\alpha^*$ = $\alpha^* D^2$ = dimensionless form of $\alpha$
$\beta$ = parameter in the Forchheimer equation [Equations (12) and (13)]
$\beta^*$ = $\beta D$ = dimensionless form of $\beta$
$\lambda$ = wavelength = length of a period of the test capillary, consisting of a narrow and a large capillary segment
$\mu$ = viscosity of fluid
$\rho$ = density of fluid
$\bar{\tau}$ = viscous stress tensor
$\phi$ = porosity

### Subscripts

$l$ = denotes large capillary segment
$s$ = denotes small capillary segment
$c$ = denotes calculated quantity
$m$ = denotes measured quantity

## LITERATURE CITED


Azzam, M. I. S., "The Effect of Geometry on ther Permeabilities of Individual Capillaries with Periodic Changes in Cross Section," M.A.Sc. thesis, Univ. of Waterloo, Ontario (1971).

Dullien, F. A. L., and V. K. Batra, in *Flow through porous media,*" pp. 1-30, Am. Chem. Soc., Washington, D.C. (1970).

Dullien, F. A. L., G. K. Dhawan, Nur Gurak, and L. Babjak, "Study of the Relationship between Pore Structure and Oil Recovery," Soc. Petrol. Engrs. J., **12**, 191 (1972).

Dullien, F. A. L., and P. N. Mehta, "Particle Size and Pore Size Distribution Determination by Photomicrographic Methods," *Powder Technol.*, **5**, 179 (1971/72).

Dullien, F. A. L., E. Rhodes, and S. R. Schroeter, "Comparative Testing of some Statistical Methods for obtaining Particle Size Distributions," *ibid.*, 3, 124 (1969/70).

Guin, J. A., D. P. Kessler and R. A. Greenkorn, "The Permeability Tensor for Anisotropic Nonuniform Porous Media," *Chem. Eng. Sci.*, **26**, 1475 (1971).

Katz, D. L., et al., *Handbook of Natural Gas Engineering*, p. 48, McGraw-Hill, New York (1959).

Scheidegger, A. E., "The Physics of Flow through Porous Media", U. Toronto Press, Canada (1957).

Slattery, J. C., "Flow of Viscoelastic Fluids through Porous Media," *AIChE J.*, **13**, 1066 (1967).

Whitaker, S., "Advances in Theory of Fluid Motion in Porous Media," *Ind. Eng. Chem.*, **61**, 14 (1969).



*Manuscript received May 16, 1972; revision received August 15, 1972; paper accepted August 18, 1972.*